The glycocalyx: a diagnostic and therapeutic target in cardiometabolic diseases

Velden, A.I.M. van der

CHAPTER 5

Supplementation with Endocalyx preserves glomerular endothelial glycocalyx and capillary stability in experimental diabetes

Anouk I.M. van der Velden
Wendy M.P.J. Sol
Angela Koudijs
Marissa L Maciej-Hulme
M. Cristina Avramut
Annemarie M. van Oeveren-Rietdijk
Mark de Graaf
Gangqi Wang
Hetty C. de Boer
Hans Vink
Johan van der Vlag
Ton J. Rabelink*
Bernard M. van den Berg*
*** Share last authorship**

Abstract

Damage to the glomerular endothelial glycocalyx is one of the various mechanisms in diabetic nephropathy. Over the years, restoring the glomerular glycocalyx has become an interesting therapeutic target, as current treatments are insufficient to slow down progression to end-stage renal disease. In the current study we investigated whether dietary Endocalyx™ suplementation (fucoidan, other glycocalyx constituents and antioxidants) is able to preserve the glomerular endothelial glycocalyx, reduce heparanase-1 (HPSE-1) activity, and affect renal myeloid cells in 8-week-old ApoE-KO mice rendered diabetic through repeated intraperitoneal streptozotocin (60mg/kg) injections with free access to cholesterol-enriched (0.15%) chow. To avoid major metabolic changes, blood glucose was kept between 15-20mmol/L. From week 12 on, mice received supplementation with Endocalyx™. Ten weeks of dietary supplementation with Endocalyx™ in diabetic mice prevented glomerular capillary damage and preserved endothelial glycocalyx coverage of both heparan sulfates and hyaluronan. While a direct HPSE-1 inactivation effect was found *in vitro*, we only observed the heparan sulfate preservation *in vivo*. Preservation was accompanied with a reduced % of CD11b positive renal cortical macrophages and dendritic cells without an effect on the major resident myeloid cell population, macrophage-like dendritic cells.

Introduction

Endothelial cell dysfunction has been implicated as a major contributor in the pathophysiology of diabetic nephropathy (DN) [1, 2]. Chronic exposure to the inflammatory diabetic environment due to circulating advanced glycation end products, reactive oxygen species (ROS) and inflammatory cytokines alters the composition and integrity of the glomerular endothelial glycocalyx. This complex network of glycoproteins, plasma proteins, proteoglycans and glycosaminoglycans maintains an important negatively charged molecular sieve as part of the glomerular filtration barrier [3]. The glycocalyx composition is highly dynamic, with a balance between biosynthesis and shedding of its constituents [4]. However, in a number of pathological conditions such as sepsis or diabetes, the composition of the endothelial glycocalyx can be altered and loses its complex structure and functional properties [5-7]. Several novel treatment strategies for DN have been developed to inhibit the influx of macrophages or glycocalyx degrading enzymes. First, by inhibiting monocyte chemoattractant protein-1 (MCP-1) activity, second by reducing heparanase-1 (HPSE-1) activity, or third by supplementing glycocalyx substituents [8-11]. Therefore, restoring the structure of the glomerular glycocalyx has become an attractive therapeutic target to improve vascular health and prevent disease progression in DN.

In the present study we investigated whether dietary supplementation with glycocalyx mimetics combined in Endocalyx™, containing fucoidan extracted from *Laminaria japonica* as the main compound with added glucosamine sulphate, hyaluronic acid, a blend of superoxide dismutase, catalase and polyphenols is able to restore the glomerular glycocalyx and reduce HPSE-1 activity in a diabetic mouse model. While glucosamine sulphate could stimulate glycocalyx restoration, by increasing N-acetyl glucosamine (GlcNAc)-driven GAG synthesis [12], it is believed that the sulphated polysaccharides in low molecular weight fucoidan with chemical structural properties analogous to HS and CS will act as a heparan sulphate mimetic [13-15]. The distinct nature of this complex sulfated polysaccharide with a backbone of primarily (1 → 3)-linked α-L-fucopyranose residues and branches of 3-linked α-L-fucopyranose residues by β-D-galactopyranose and 3-linked α-L-fucopyranose residues by non-reducing terminal fucose units [16] was further investigated *in vitro* on endothelial glycocalyx restoration [14] and reducing HPSE-1 activity and an *in vivo* experimental glomerulonephritis study [15].

Materials and Methods

Cell culture and treatment

Murine glomerular endothelial cells (mGEnCs) were cultured as described previously [17]. Human Renal Glomerular Endothelial Cells (HRGECs, ScienCell, Uden, The Netherlands)

were cultured on fibronectin (Promocell, Heidelberg, Germany) coated flasks (COSTAR, Amsterdam, The Netherlands) between passage 2-5 with Endothelial Cell Medium (1001, ScienCell) supplemented with 5% FBS (0025, ScienCell), 1% Endothelial Cell Growth Supplement (1052, ScienCell) and 1% Penicillin/Streptomycin (0503, ScienCell) in 5% CO_2 at 37^{o}C [18]. Where indicated, cells were treated with 1 µg/mL LPS O111:B4 (Sigma, Houten, The Netherlands, Cat# L2630) and/or 1-2 µg/mL *L. japonica* fucoidan (≥90%, gift from MicroVascular Health Solutions) for 12-24 hours.

HS release competition ELISA and competition ELISAs to detect Fucoidan

Nunc MaxiSorp™ 96- well ELISA plates (Thermo Scientific) were coated with either 10 µg/mL heparan sulphate from bovine kidney (Sigma) or chondroitin sulphate-A (CS-A) (Iduron) in coating buffer overnight at room temperature in a humidified chamber. Plates were washed 5x with PBS/0.05% Tween20 (PBST) and blocked with 1% bovine serum albumin (Sigma) for 2 hours. 0-4 µg/mL fucoidan (gift from MicroVascular Health Solutions LLC, Alpine, UT, USA) was pre-incubated with glycosaminoglycan antibodies: anti-HS (F58-10E4) (1:100, Amsbio), anti-CS single chain fragment variable (ScFv) I03H10 (1:100), anti-HS (JM403) (1:5000, Amsbio) for 1 hour. Fucoidan/antibody mixtures were then incubated with glycosaminoglycan-coated ELISA plates for 1 hour. Plates were washed 5x PBST and incubated with secondary antibodies: goat anti-mouse IgM-HRP (1:5000, Southern Biotech), mouse anti-VSV-G-peroxidase (1:2000, Sigma). Plates were washed 5x PBST and colour was developed with 1x tetramethylbenzidine ELISA substrate solution (Invitrogen). Absorption was measured at 450 nm.

Immunocytochemistry

Cells were cultured in Nunc™ Lab-Tek™ Flask on Slide chambers (170920, Thermo Scientific, Landsmeer, The Netherlands) until confluent, then treated with LPS for 24 hours. Selected cultures were also subjected to fucoidan treatment for the final 12 hours of LPS stimulation. Cells were washed twice with PBS and fixed with 4% paraformaldehyde in PBS for 10 mins at RT. Fixed slides were washed five times with PBS and then blocked with 0.2% BSA for 1 hour at RT. Appropriate sections were incubated with primary mouse anti-rat IgM HS antibody JM403 (1.3 µg/mL) diluted in 0.2% BSA, followed by Alexa Fluor IgM-488κ (1:500, Life Technologies, Bleiswijk, The Netherlands) for 1h each time. Slides were washed between antibodies three times for 10 mins in PBST. Slides were mounted in Vectorshield mounting medium H-1000 with DAPI (Vector Labs Inc., Burlingame, CA, USA) and sealed with a glass coverslip. Images were collected using a Zeiss Axio imager M1 (Zeiss, Breda, The Netherlands) immunofluorescence microscope.

Diabetic apoE KO mouse model

Six-week-old male B6.129P2-*Apoe*^{tm1Unc}/J mice (ApoE-KO; The Jackson Laboratory, Bar Harbor, ME) were rendered diabetic through intraperitoneal injections of 60mg/kg strep-

tozotocin (STZ; Sigma-Aldrich, St. Louis, MO) for 5 consecutive days, as described before [11] (supplemental figure 1A). Control ApoE-KO mice were injected with citrate buffer alone and were used for baseline measurements. All mice had free access to standard rodent diet (NC; Ssniff Spezialdiäten GmbH, Soest, Germany). At week 8, diabetic mice were fed cholesterol enriched (0.15%) chow until the end of the study. At week 11, diabetic mice were randomized into two groups; a diabetic group (diabetes) and a diabetic group that received Endocalyx™ supplementation (US patent # 9943572; MicroVascular Health Solutions LLC, Alpine, UT, USA) starting at week 12. Estimated daily dosage calculations of Endocalyx™ supplement (Endocalyx) per animal (in mg) is: fucoidan sulphate 0.12, hyaluronic acid 0.02, glucosamine-SO_4 0.43 and oxxynea OMD-SOD 0.14 which relates to the recommended daily dose in humans of: 425-, 70-, 1500- and 480mg, respectively. Blood glucose concentrations by tail-tip blood droplets were measured with an Accu-check glucose meter (Roche, Basel, Switzerland). When glucose concentrations exceeded 20 mmol/L, mice were treated with 1–2 units insulin (Lantus, Aventis Pharmaceuticals, Bridgewater, NJ, US) up to three times per week. Mice were sacrificed at week 22 of age. Animal experiments were approved by the Ethical Committee on Animal Care and Experimentation of the Leiden University Medical Center (permit no. AVD1160020172926). All work with animals was performed in compliance with the Dutch government's guidelines.

Urine collection and analysis

Mice were weighted before and after residing in the metabolic cage (Techniplast S.p.a, Buguggiate, Italy) and water- and food intake, and urine were collected. After acclimatization, 14hrs-urine was collected at week 11, -17 and -21. Urine samples were centrifuged to remove debris and stored at -20°C. Urinary albumin concentrations were quantified with an enzyme-linked immunosorbent assay (ELISA; Bethyl Laboratories, Inc. Montgomery, TX, USA) and creatinine concentrations were quantified by the Jaffe´ method using 0.13% picric acid and a creatinine standard set (Sigma-Aldrich, Merck Life Science NV, Amsterdam, The Netherlands). Urine MCP-1 activity was measured with an immunoassay according to the manufacturer protocol (R&D Systems Europe, Ltd., Abingdon, UK). Urinary HPSE-1 activity was measured (Takara Bio Inc., Shiga, Japan). Urine samples were run through Zeba™ Spin Desalting Columns (ThermoFisher Inc., Waltham, MA, USA) for removal of salts and other small molecules (<1000 MW) before HPSE-1 activity detection. Excretion of urinary kidney injury molecule-1 (KIM-1) was determined with an ELISA kit (R&D Systems, Minneapolis, MN, USA). Optical densities for albumin, creatinine, MCP-1, HPSE-1 activity and KIM-1 were measured with an ELISA plate reader.

Tissue preparation and histology

Mice were anesthetized by isoflurane inhalation and perfused via the left ventricle with HEPES-buffered salt solution containing 0.5% bovine serum albumin and 5 U/mL heparin to remove blood. After removal of the capsules, one half of the right kidney was fixed in

paraformaldehyde (PFA) solution (4%) for 1 to 2 hours and processed further for endothelial glycocalyx coverage while the other half was frozen in liquid N_2 and stored at -80°C. Both halves of the left kidney were placed in 2% PFA in PBS overnight at 4°C, followed by paraffin embedding for periodic acid-Schiff (PAS), methenamine silver-periodic acid-Schiff (MPAS) or immunofluorescence staining.

A subset of mice (n = 3/group) were anesthetized, the abdominal aorta was exposed and cannulated adjacent to the left renal artery. The right renal artery was ligated at the renal stalk after which the left kidney was perfused with 5mL Hanks-buffered salt solution (HBSS, Gibco) containing 0.5% BSA (Sigma, A7030, essentially globulin free) and 5IU/mL heparin at 2mL/minute to remove blood, followed by 2mL of cationic ferritin (horse spleen, 2.5mg/mL, Electron Microscopy Sciences, Fort Washington, PA) in HBSS at 2mL/minute. The left kidney was excised, its capsule removed, and stored in fixative, 1.5% glutaraldehyde (GA) and 1% PFA (both from Electron Microscopy Sciences, Hatfield, PA) in 0.1M sodium-cacodylate buffered solution (pH 7.4), overnight at 4°C for further processing for transmission electron microscopy (TEM). Of another subset of mice, the left kidney was placed in PBS on ice for single cell isolation for FACScan analysis.

Glomerular endothelial coverage

Glomerular endothelial glycocalyx coverage was determined using fluorescently labelled lectin Lycopersicon esculentum (LEA-FITC) and the N terminus rat neurocan construct of the HA-specific neurocan-dsRed (Ncan-dsRed) construct, as described previously [2, 3]. In short, overnight PFA fixed tissue was subsequently sectioned in 100µm thick slices with a Leica VT1000S vibratome (n = 3/group) and submerged in HBSS (Life Technologies Europe BV, Bleiswijk, The Netherlands) containing 0.5% BSA, 5 mmol/L HEPES, and 0.03 mmol/L EDTA (HBSS-BSA). Slices were incubated with 10µg/mL of fluorescently labeled Lycopersicon esculentum (LEA) or Ncan-dsRed [2] to visualize the glycocalyx, together with 5µg/mL monoclonal mouse anti-mouse CD31 antibody (Ab28364, Abcam, Cambridge, MA) to identify the endothelial cell membrane, overnight at 4°C on a shaker (in dark). After 3 washes with HBSS-BSA slices were incubated for 2 hrs with 10µg/mL Alexa Fluor-568, or AF488–conjugated goat anti-mouse IgG (Molecular Probes, Grand Island, NY) and Hoechst 33528 (Sigma-Aldrich, 1:2000) at 4°C on shaker (in dark). Slices in HBSS-BSA were fixated between glass slide and coverslip in mounting medium and imaged on a LEICA TCS SP8 X WLL microscope (Leica, Rijswijk, The Netherlands) and a 40x objective (HC PL APO CS2 40x/1.30 OIL, Leica). Sequential 16-bit confocal images (xyz dimensions, 0.142 x 0.142 x 0.3 µm) were recorded using LAS-X Image software (Leica). The endothelial glycocalyx was quantified by calculating the distance from the peak of the CD31 signal to the half-width of the intraluminal lectin signal along a line of interest, using intensity profiles (ImageJ).

Cationic ferritin determination with TEM

Cationic ferritin perfused tissue, stored in fixative, 1.5% GA and 1% PFA in 0.1M sodium-cacodylate buffered solution, was subsequently sectioned in 180µm thick slices with a Leica VT1000S vibratome, rinsed 2x with 0.1M sodium cacodylate-buffered solution, and post-fixated for 1hr with 1% osmium tetroxide (Electron Microscopy Sciences) and 1.5% potassium ferrocyanide in demineralized water [2, 3]. Samples were further washed, dehydrated in ethanol, infiltrated with a mixture of epon LX-112 and propylene oxide (1:1) for 1 hr, followed by pure epon for 2hrs, embedded in epon mounted in BEEM capsules (Agar Scientific, Essex, United Kingdom) and polymerized for 48hrs at 60°C. 100nm Thick sections were cut using a diamond knife (Diatome, Biel, Switzerland), collected on single slot copper grids covered with formvar film and carbon layer, and then stained with 7% uranyl acetate in demineralized water for 20 minutes, followed by Reynold's lead citrate for 10 minutes. Data was collected at an acceleration voltage of 120kV on a Tecnai G2 Spirit BioTWIN transmission electron microscope (TEM), equipped with an FEI 4k Eagle CCD camera. Virtual slides were acquired with 18,500x magnification at the detector plane, corresponding to a 1.2nm pixel size at the specimen level. Representative capillary sections of each recorded glomerulus (n = 1/group) from virtual slides were selected for high resolution imaging.

Immunohistochemistry

Deparaffinized kidney sections (4µm thick) were washed in PBS and antigen retrieval was performed in a citrate buffer (Dako S1699, pH 6.0) in an autoclave, blocked with serum-free protein block (Dako X0909) for 1 hour at room temperature. Sections were incubated overnight at 4°C with primary mouse anti-HS antibodies (clone JM403, AMS-Biotechnology, Bioggio-Lugano, Switzerland) or with fluorescently labeled Lycopersicon esculentum (LEA-FITC), in combination with mouse pan-endothelial cell marker (BD Biosciences, San Jose, CA), followed by corresponding fluorescent-labelled secondary antibodies for 1 hour at 4°C, all in blocking buffer. Another set of sections were incubated overnight at 4°C with primary polyclonal rabbit antibodies against HPSE-1 (InSight Biopharmaceuticals, Rehovot, Israel) in combination with rat monoclonal antibodies against mouse F4/80 (ab6640, Abcam, Cambridge, MA) and polyclonal goat antibodies against mouse nephrin (AF3159, R&D Systems), followed by corresponding fluorescent-labelled secondary antibodies for 1 hour at 4°C, all in blocking buffer. Slides were embedded in Prolong™ gold antifade mountant with DAPI (P36931, Thermofisher). Fluorescent images of the slides were recorded using a 3D Histech Pannoramic MIDI Scanner (Sysmex, Etten-Leur, the Netherlands). Annotated glomeruli (± 50/sample) were exported for further analysis in the public domain NIH ImageJ software (http://rsb.info.nih.gov/ij). Fluorescence of the exported 16-bit images were analysed using a macro using the auto threshold function based on the isodata algorithm [19] to generate glomerular surface area, mean fluorescence and % positive

area which are used to calculate total glomerular fluorescence (surface area x (% positive area/100)) x mean fluorescence (mean FL x μm^2).

Single cell isolation for FACscan

Left kidneys placed in PBS on ice for FACScan analysis were cut in small pieces and placed in a 6-well plate containing 1mL of collagenase type 1A (1.6mg/mL) and DNAse (60U/mL) in sterile H_2O and incubated for 30 min at 37°C (5% CO_2 incubator with intermittent agitation). Tissue, including liquid, was transferred on a 100µm cell strainer, placed on a 50 mL tube and was passed through the strainer using the plunger of a 2.5 ml syringe to crush the tissue further and cell strainer is flushed twice with 10mL DPBS at rT. The fall through is transferred to a 40µm cell strainer and passage is repeated, followed by centrifugation for 5 min at 1500rpm (rT). Supernatant was discarded and cells were suspended in 5mL ice-cold shock buffer and incubated for 3-4 min on ice. At least 5mL ice-cold DPBS was added, followed by centrifugation for 5 min at 1500rpm (4°C). Supernatant was discarded cells were suspended in FACS buffer on ice.

Staining protocol for FACScan

Appropriate volumes of adjusted cells (equivalent to 1.0 x 10^6cells) were pipetted into each tube and appropriate volume of the conjugated antibodies directed to the cell surface marker(s) of interest were added. Per sample 4 cocktails were used (supplemental table 1). Each tube was vortexed gently to mix cells with antibodies, and incubated for 15 minutes in the dark at rT. Reagent A (100µL 1% PFA solution) was added and incubated for 15 minutes at rT, washed once in 1mL FACS buffer (FB; 1% BSA 0.01% NaAz in PBS). Centrifuged for 5 minutes at 5000 rpm, supernatant was aspirated and vortexed to fully resuspend the cell pellet. Reagent B (100 µl Permeabilization Medium) was added together with recommended volume of conjugated intracellular antibodies. Vortexed for 1-2 seconds and incubated for 20 minutes, washed once in 1 mL FB. Centrifuged for 5 minutes at 5000 rpm and supernatant was aspirated. Cells were resuspended in 200µL of 0.1% PFA fixative solution for storage at 2-8°C in the dark and analyzed within 24 hours. Samples were measured on a Cytek Aurora 5 flow cytometer (Cytek Biosciences B.V., Amsterdam, The Netherlands), according to manufacturer's guidelines. Characterization of HPSE-1 and cathepsin L positive kidney myeloid cells was based on the antibody cocktails as shown in supplemental table 1. Gating strategy after life/dead discrimination and gating for single cell as shown in supplemental figure 2. In short, first cells positive for CD11b were gated and selected on cell size. Next, MHC-II positive cells were selected (excluding, e.g. naïve monocytes, NK cells, neutrophils and basophils), finishing with selection of the myeloid cell-types based on CD11c and F4/80 expression, and CD370 and Cx3CR1 expression: macrophages (Mϕ; $CD11c^{neg}$/$F4\text{-}80^{hi}$/MHC II^{lo}/$CD11b^{lo}$/$CD370^{lo}$/$CX3CR1^{hi}$), dendritic cells (DC) switched to a macrophage-like phenotype [20] (DC/Mϕ-like; $CD11c^{lo}$/$F4\text{-}80^{hi}$/

MHC II^{hi}/CD11b^{lo}/CD370^{hi}/CX3CR1^{hi}) and DCs (CD11c^{hi}/F4-80^{neg}/MHC II^{hi}/CD11b^{hi}/CD370^{hi}/CX3CR1^{lo}).

Statistical analysis

Data are presented as means with standard deviation (SD). Urine production, albumin-to-creatinine ratio (ACR) and urinary HPSE-1 activity during treatment were analyzed by using linear mixed models with Bonferroni post hoc test. This takes into account that samples over time from the same animal are not independent. Differences per timepoint between groups were analyzed by ANOVA with Tukey's post-hoc test. The ACR and urinary HPSE-1 activity were log-transformed before the ANOVA and linear mixed model analysis.

Differences in other experiments were determined using analysis of variance and post hoc analyses with Tukey's multiple comparison test. Comparison of expression between two different groups was evaluated using a t-test. Statistical analyses were performed using SPSS statistical software version 25 (SPSS Inc., Chicago, IL) and GraphPad Prism version 8 (GraphPad Inc., La Jolla, CA). A significance level of 0.05 was considered statistically significant.

Results

Fucoidan from *Laminaria japonica* inhibits heparanase activity *in vitro*

First, we tested the possible HPSE-1 inhibitory effects of fucoidan, one of the main components of the Endocalyx^{TM} supplement. Previously it has been shown that orally administered fucoidan, through intestinal uptake, in healthy volunteers can be detected in blood with peak levels around 50ng/mL (intake of 1 gram) at 6 hours in its unchanged form, while at 9 hours, fractions can be observed in urine samples [21, 22]. To measure fucoidan levels, we evaluated anti-HS antibodies i.e. F58-10E4 and JM403, respectively [10], and anti-CS antibody via IO3H10 [23] for binding to fucoidan. Anti-HS antibody binding of clone F58-10E4 to fucoidan resulted in a binding ratio of 29.5ng per ng antibody and for the anti-CS antibody, clone IO3H10, of 0.04ng per ng of antibody (supplemental figure 2A-F and supplemental table 1). No binding of the anti-HS antibody clone JM403 to fucoidan was observed (supplemental figure 2G and supplemental table 1). Therefore, we used this antibody to evaluate the inhibitory effect of fucoidan on recHPSE-1 activity. Results revealed a concentration dependent reduction up to about 90% by 10ng/mL fucoidan (figure 1A). In LPS activated murine glomerular endothelial cells (mGEnCs) active HPSE-1 release could be inhibited in the presence of 10ng/mL fucoidan (figure 1B). In addition, fucoidan was also able to protect the endothelial glycocalyx by reducing the release of HS into the extracellular milieu in both murine and human derived glomerular endothelial cells (figure 1C, D).

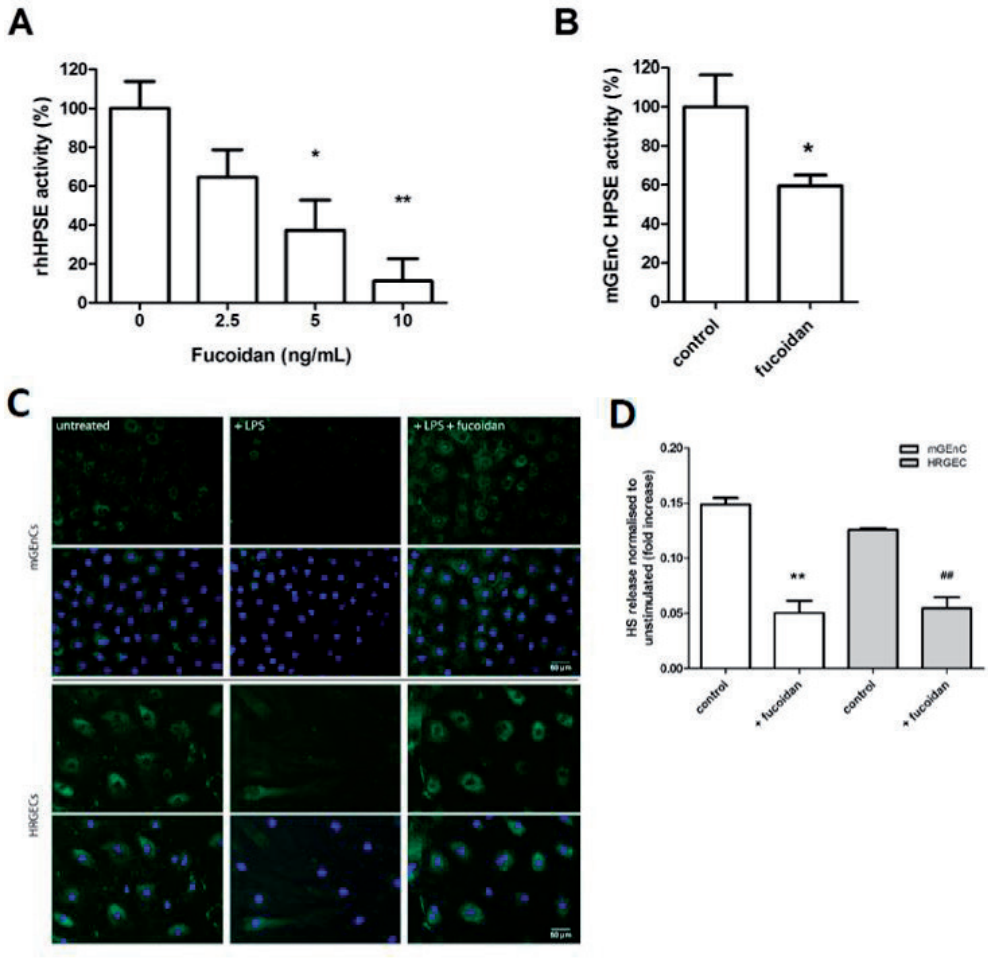

Figure 1. Fucoidan inhibits HPSE-1 activity and protects endothelial surface glycocalyx. (A) Dose-dependent inhibition of recombinant HPSE-1 (rhHPSE-1). rhHPSE activity in presence of 0-10 ng/mL fucoidan was measured by an indirect ELISA. Data significance was analyzed using a one-way ANOVA with Dunnett's post-hoc comparison. *P < 0.05, **P < 0.01 (B) Mouse glomerular endothelial cells (mGEnCs) were treated with LPS to induce the release of active HPSE into the media. Medium HPSE-1 activity was measured in presence and absence of 10 ng/mL fucoidan (n=3). Data significance was analyzed using an unpaired t-test. *P < 0.05 Loss of endothelial heparan sulfate (HS) glycocalyx was measured (C) via immunocytochemistry using anti-HS JM403 and (D) by competition ELISA of HS release into cell media in both mGEnCs and human renal glomerular EC (HRGECs). In the presence of 10 ng/mL fucoidan, endothelial HS glycocalyx was preserved and release of HS was significantly reduced (n= 3). JM403, green; DAPI, blue. Data significance was analyzed using an unpaired t-test. **P < 0.01, LPS-stimulated mGEnCs + fucoidan vs. LPS-stimulated mGEnCs, $^{\#\#}P$ < 0.01, LPS-stimulated HRGECs + fucoidan vs. LPS-stimulated HRGECs.

Diabetes induced ApoE-KO mice

At week 11 (before randomization in diabetes or Endocalyx™ groups), diabetic mice manifested with hyperglycemia, weight loss, polyuria, albuminuria and increased urinary HPSE-1 activity levels (supplemental figure 1B,C). Following the intervention period (week 12-22), high blood glucose levels in diabetic mice were maintained at preferred set glucose levels (15-20 mmol/L) through regular insulin administration to prevent glucotoxicity and a metabolic shift to overt lipid use for energy in these animals (supplemental figure 1D).

Supplementation of glycocalyx mimetics protects the glomerular glycocalyx

We investigated whether 10 weeks of Endocalyx™ supplementation could preserve the glomerular glycocalyx by staining PFA fixed renal sections directly with the fluorescently labelled lectin *Lycopersicon esculentum* (LEA-FITC) (figure 2A). Diabetes reduced the intraluminal endothelial surface lectin thickness, and coverage, to 0.157 µm, compared to 0.272 µm in control mice (difference 0.117 µm 95% CI 0.059 - 0.175) (figure 2B,C). Endocalyx™ supplementation during the 10-week intervention prevented this glycocalyx degradation revealing a 0.227 µm thick layer (difference 0.070 µm compared to diabetes group, 95% CI 0.012 - 0.128). Similarly, staining specifically for hyaluronan, using Ncan-dsRed, revealed protection upon supplementation with Endocalyx™ (figure 2D-F). This endothelial surface layer preservation was further confirmed by visualizing glomerular intraluminal endothelial cationic ferritin coverage (figure 2G). Cationic ferritin was present at the luminal endothelial cell surface, within the fenestrae and underneath the endothelium. In contrast, disruption of the cationic ferritin coverage alongside the luminal endothelial cell surface could be seen in the glomerulus of diabetic mice (figure 2G, middle panel). Total glomerular tuft staining on paraffin embedded sections with LEA-FITC revealed no significant differences in expression between control and both diabetic groups (with or without Endocalyx™), which was corroborated by glomerular tuft heparan sulfate detection using JM403 antibodies (figure 2H,I).

Endocalyx™ supplementation prevents glomerular capillary rarefaction

STZ induction of diabetes combined with a cholesterol-enriched diet (0.15%), resulted in minimal glomerular changes after 16 weeks, as shown by PAS and MPAS stained examples (figure 3A) but a significant reduced number of capillaries per glomerulus in diabetic mice compared to controls (difference of -4.2 95% CI -5.8 - -2.6) was observed (figure 3B). The number of capillaries per glomerulus in diabetic mice supplemented with Endocalyx™ remained equal compared to control (difference of 2.9 95% CI 1.4 - 4.5). No changes were observed in capillary surface- and mesangial surface area (figures 3C,D).

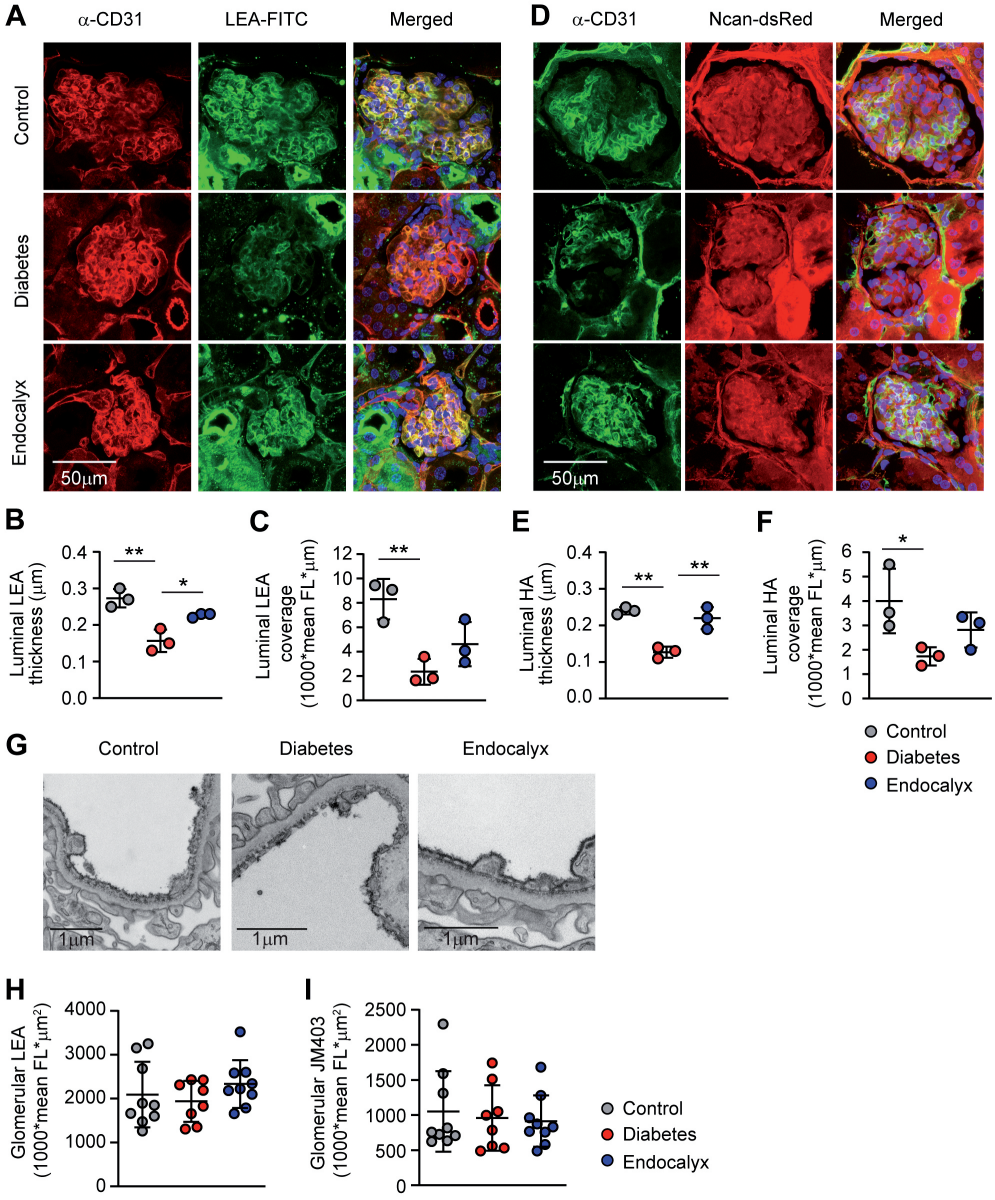
A
α-CD31
LEA-FITC
Merged
Control
Diabetes
Endocalyx
50μm
D
α-CD31
Ncan-dsRed
Merged
50μm
B
Luminal LEA thickness (μm)
C
Luminal LEA coverage (1000*mean FL*μm)
E
Luminal HA thickness (μm)
F
Luminal HA coverage (1000*mean FL*μm)
Control
Diabetes
Endocalyx
G
Control
Diabetes
Endocalyx
1μm
H
Glomerular LEA (1000*mean FL*μm²)
I
Glomerular JM403 (1000*mean FL*μm²)
Control
Diabetes
Endocalyx

Figure 2. Glomerular endothelial glycocalyx coverage (A) Representative images of direct glycocalyx staining using fluorescent labeled lectin *Lycopersicon esculentum* (LEA-FITC) and anti-CD31 antibodies for endothelial cell detection; scale bar 50µm. Reduction of **(B)** the luminal glycocalyx (LEA) thickness and **(C)** luminal glycocalyx (LEA) coverage, assessed in a subset of n = 3 control- (grey), diabetic- (red) and diabetic ApoE-KO mice after Endocalyx intervention (blue). **(D)** Representative images of direct glycocalyx staining using fluorescent labeled neurocan (Ncan-dsRed) and anti-CD31 antibodies for endothelial cell detection; scale bar 50µm. Reduction of **(E)** the luminal glycocalyx (Ncan-dsRed) thickness and **(F)** luminal glycocalyx (Ncan-dsRed) coverage, assessed in a subset of n = 3 control- (grey), diabetic- (red) and diabetic ApoE-KO mice after Endocalyx intervention (blue). **(G)** Representative transmission electron micrographs of cationic ferritin-stained glomerular endothelial surfaces in control-, diabetic- apoE-KO and Endocalyx intervention; scale bars 1µm. Quantification of total glomerular immunofluorescence staining of **(H)** lectin *Lycopersicon esculentum* (LEA-FITC) and **(I)** heparan sulfate (clone JM403). Analysis was performed on ± 50 glomeruli per sample in control- (n = 9), diabetic- (n = 8) and diabetic apoE-KO mice after Endocalyx intervention (n = 9). Values are given as mean with standard deviation. Differences between groups were assessed by ANOVA with Tukey's post-hoc test: $*P < 0.05$, $**P < 0.01$.

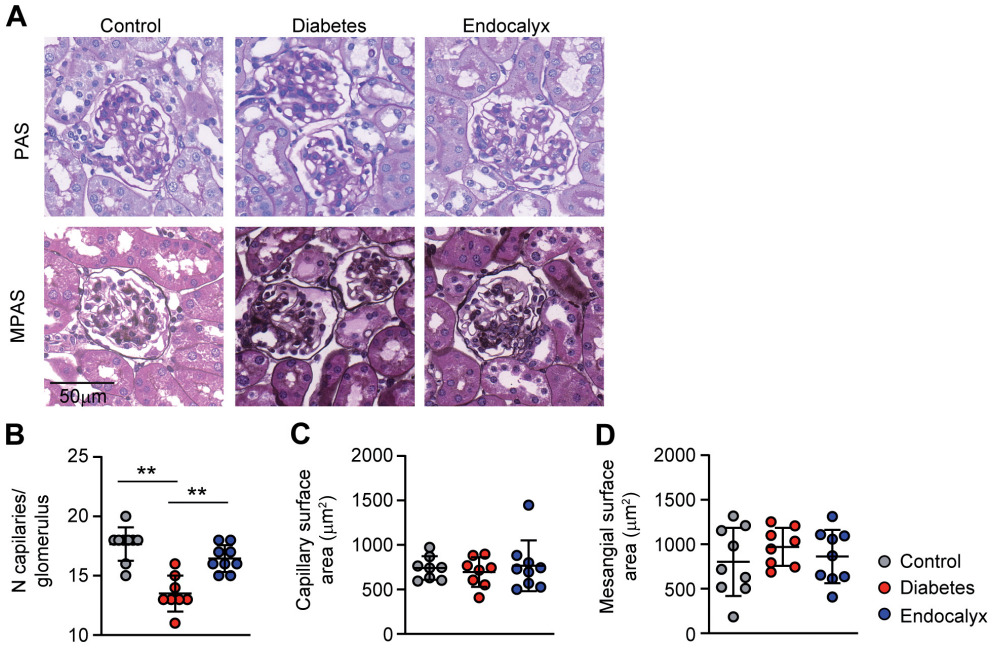

Figure 3. Histological glomerular changes. **(A)** Representative images of periodic acid–Schiff (PAS, top) and (methenamine silver-periodic acid-Schiff (MPAS, bottom) stained glomeruli of control- (left), diabetic- (middle) and diabetic apoE-KO mice with Endocalyx™ supplement (right); scale bar, 50 µm. Quantification of **(B)** number of capillaries per glomerulus, **(C)** glomerular capillary- and **(D)** mesangial surface area. Analysis was performed on ± 50 glomeruli per sample in control- (grey, n = 9), diabetic- (red, n = 8) and Endocalyx intervention (blue, n = 9). Values are given as mean with standard deviation (SD). Differences between groups were assessed by ANOVA with Tukey's post-hoc test: $^{**}P < 0.01$.

Urinary markers and renal HPSE-1 staining after Endocalyx™ supplementation

While at week 11 diabetic mice had elevated albumin-to-creatine ratios (ACR), throughout the rest of the experiments, in the glucose controlled setup, ACR tended to decline over time in parallel to urine production in both diabetic groups (figure 4A). This tendency precluded identifying an isolated effect of glycocalyx restoration on albuminuria. Meanwhile, no differences in urinary HPSE-1 activity were observed during the intervention period, as exemplified by similar trends in both groups between week 11 and 21 (figure 4B). In addition, urinary KIM-1 and MCP-1 levels did not change or remained below threshold levels for detection in both diabetic groups when compared to control non-diabetic mice (data not shown). Total glomerular HPSE-1 (inactive and active) staining on paraffine embedded sections, mostly corresponded with podocyte nephrin-1 staining and was not significantly changed after the intervention period in comparison to the non-diabetic control group (figures 4C,D). Although peritubular F4/80 positive cells were detected, no clear F4/80 positive stained cells were observed within the glomeruli (data not shown).

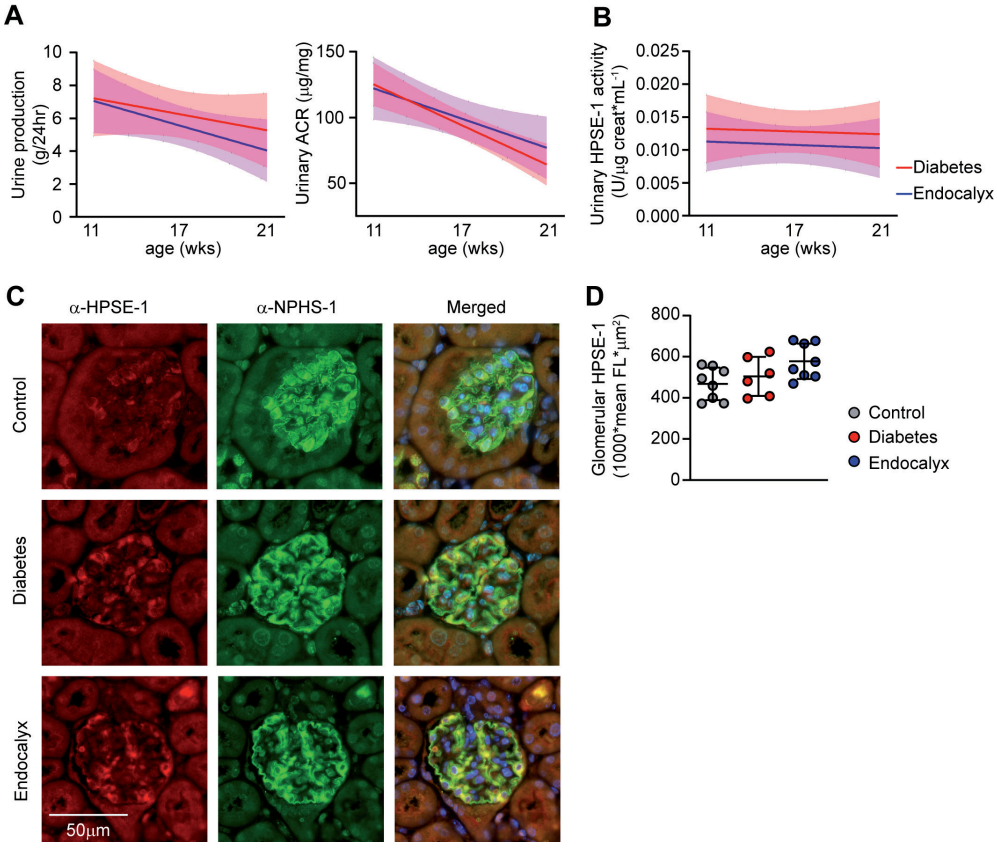

Figure 4. Urinary albumin levels and HPSE-1 activity. Trends in urine production and albumin-to-creatinine ratio (ACR) **(A)** between diabetic- (n = 8) and diabetic apoE-KO mice after Endocalyx intervention (n = 9) over time. Trend in urinary HPSE-1 activity **(B)** between diabetic- (n = 8) and diabetic apoE-KO mice after Endocalyx intervention (n = 9) over time. **(C)** Representative images of glomerular HPSE-1 (red) and nephrin-1 (NPHS-1, green) protein expression in control- (top panels), diabetic- (middle panels) and diabetic apoE-KO mice with Endocalyx™ supplement (bottom panels); scale bar 50 µm.), **(D)** Quantification of total HPSE-1 protein expression. Analysis was performed on ± 50 glomeruli per sample in control- (n = 9), diabetic- (n = 8) and diabetic apoE-KO mice with Endocalyx™ supplement (n = 9). Values are given as mean with standard deviation (D). Differences between groups were assessed by unpaired t-test (D) and simple linear regression (A,B): $*P < 0.05$

Changes in renal myeloid cells in HPSE-1 and cathepsin L expression after supplementation of glycocalyx mimetics

Since pilot immunofluorescence experiments on renal cathepsin L expression revealed very high expression levels in the various epithelial cells, masking possible cathepsin L positivity of myeloid cells (data not shown), we decided to study single myeloid cells with flow cytometry. To investigate renal myeloid cell presence, total kidney single cells were isolated and myeloid cells were determined using a gating strategy shown in supplemental

figure 3A using the antibody cocktails in supplemental table 2, in part according to Cao, *et al.* [24]. The three major myeloid cell types observed were macrophages (Mϕ; CD11c^{neg}/F4-80^{hi}/MHC II^{lo}/CD11b^{lo}/CD370^{lo}/CX3CR1^{hi}), dendritic cells (DC; CD11c^{hi}/F4-80^{neg}/MHC II^{hi}/CD11b^{hi}/CD370^{hi}/CX3CR1^{lo}) and DC switched to a Mϕ -like phenotype [20] (DC/Mϕ-like; CD11c^{lo}/F4-80^{hi}/MHC II^{hi}/CD11b^{lo}/CD370^{hi}/CX3CR1^{hi}), of which the DC/Mϕ-like cell population was found to be about 10 times more present compared to either Mϕ or DCs (figure 5A). Without obvious differences in phenotype differentiation (mean fluorescence intensities) between the diabetes and Endocalyx group (supplemental figure 3B), the percentage of the total CD11b positive population of both Mϕ and DCs were lower in the Endocalyx group compared to the diabetes group (Mϕ: 5 ± 1 vs. 9 ± 2, p = 0.020 and DC: 5 ± 1 vs. 9 ± 3, p = 0.037, respectively; and figure 5B). The DC/ Mϕ-like cell population did not differ between the two groups (77 ± 4 vs. 70 ± 12, Endocalyx and diabetes group, respectively). In neither myeloid cell population tested could a clear cathepsin L expression level be observed (figure 5C), whereas all three cell populations were positive for HPSE-1, however, without differences between the diabetes and Endocalyx group (figure 5D).

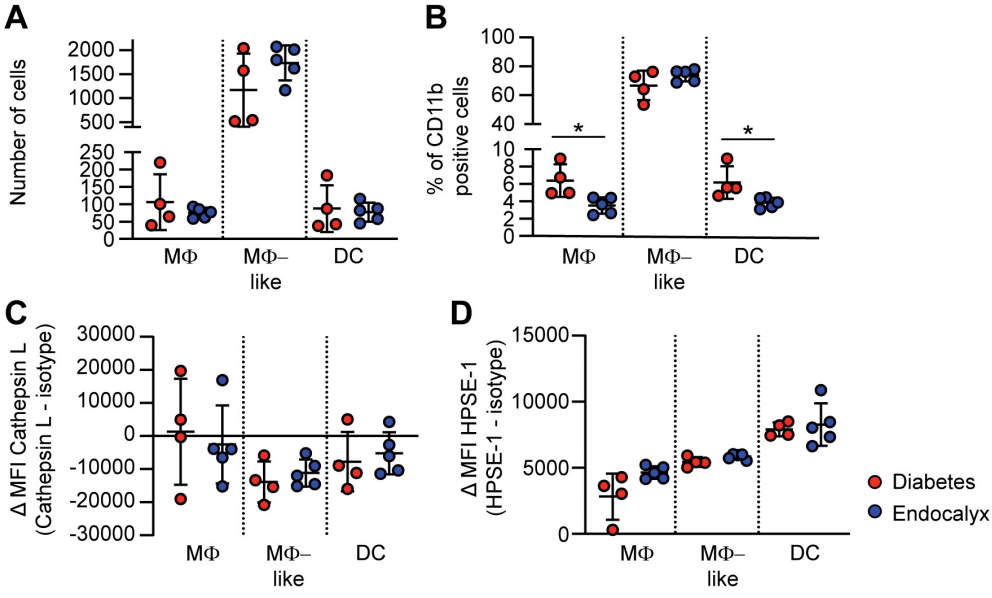

Figure 5. Cytometry of isolated kidney myeloid cells. Isolation from total kidney samples revealed three populations of myeloid cells; macrophages (Mϕ), dendritic cells (DC) switched to Mϕ-like cells and DC in **(A)** number of cells and **(B)** % of CD11b positive cells. Cell type specific expression of **(C)** cathepsin L and **(D)** the heparan sulfate degrading enzyme heparanase (HPSE-1) as function of their respective iso-type controls (ΔMFI), see Table 1. Values are given as mean with standard deviation. Differences between groups were assessed by unpaired t-test: *P < 0.05

Discussion

In the present study, we show that 10 weeks of dietary supplementation with Endocalyx™ preserved the glomerular endothelial glycocalyx coverage in diabetic ApoE-KO mice and prevented glomerular capillary rarefaction. While the main component of Endocalyx™, fucoidan, is able to inhibit HPSE-1 activity and protect the endothelial glycocalyx by reducing the release of heparan sulphate GAGs, no additional effect was found in the glomeruli. Glomerular HPSE-1 expression was predominantly colocalized with podocytes and urinary HPSE-1 activity remained stable throughout the experimental period. While no glomerular macrophages were detected, the percentage of macrophages and dendritic cells within the total CD11b positive cell population isolated from the cortex was found to be lower in the Endocalyx group.

Preventing uncontrolled gluco-toxic effects in the present STZ-induced diabetic mouse model, through regular insulin administration to keep blood glucose levels between 15-20 mmol/L, inadvertently seemed to induce a much milder pathology than we observed previously [10, 11]. This resulted in undetectable urinary kidney damage markers (KIM-1 and MCP-1) and glomerular increased presence of HPSE-1 and cathepsin L. However, glomerular endothelial changes such as loss of the luminal glycocalyx and capillary rarefaction could still be observed [10, 11, 25]. Interestingly, Endocalyx™ supplementation resulted in a shift in the percentage of macrophages and dendritic cell populations, when testing direct isolated single renal myeloid cell populations. Although the major myeloid cell population, macrophage-like dendritic cells did not change, this reduced presence of Mϕ and DCs could reflect a lower renal inflammation status upon Endocalyx™ supplementation.

We did show preservation of the glomerular capillary loops and endothelial glycocalyx coverage after Endocalyx™ supplementation. In line with the specific fucoidan data in the present study, we recently could prove that fucoidan was not only able to block HPSE-1 activity but that surface glycocalyx of primary human lung- and glomerular endothelial cells in the presence of sera from intensive care unit COVID-19 patients was preserved, preventing increased permeability and a hypercoagulable surface [14]. In these experiments fucoidan bound to the endothelial surface, inhibited the inflammatory phenotype and completely restored the endothelial barrier properties and the coagulation disorder. Similar findings were observed on endothelial glycocalyx perturbation using serum of chronic kidney disease patients with elevated uremic toxins [26], relieving arterial stifness in a mouse model of aged animals [27] and in a glomerulonephritis model [15].

In conclusion, we showed that in the diabetic mouse glomerulus, dietary supplementation with Endocalyx™ was able to prevent capillary damage and glycocalyx degradation.

References

1. Nakagawa, T., et al., *Endothelial dysfunction as a potential contributor in diabetic nephropathy.* Nat Rev Nephrol, 2011. **7**(1): p. 36-44.
2. van den Berg, B.M., et al., *Glomerular Function and Structural Integrity Depend on Hyaluronan Synthesis by Glomerular Endothelium.* J Am Soc Nephrol, 2019. **30**(10): p. 1886-1897.
3. Dane, M.J., et al., *Glomerular endothelial surface layer acts as a barrier against albumin filtration.* Am J Pathol, 2013. **182**(5): p. 1532-40.
4. Wang, G., et al., *Shear Stress Regulation of Endothelial Glycocalyx Structure Is Determined by Glucobiosynthesis.* Arterioscler Thromb Vasc Biol, 2020. **40**(2): p. 350-364.
5. Nussbaum, C., et al., *Early microvascular changes with loss of the glycocalyx in children with type 1 diabetes.* J Pediatr, 2014. **164**(3): p. 584-9 e1.
6. Wang, G., et al., *Endothelial Glycocalyx Hyaluronan: Regulation and Role in Prevention of Diabetic Complications.* Am J Pathol, 2020. **190**(4): p. 781-790.
7. Potter, D.R., et al., *Perturbed mechanotransduction by endothelial surface glycocalyx modification greatly impairs the arteriogenic process.* Am J Physiol Heart Circ Physiol, 2015. **309**(4): p. H711-7.
8. Yung, S., et al., *Sulodexide decreases albuminuria and regulates matrix protein accumulation in C57BL/6 mice with streptozotocin-induced type I diabetic nephropathy.* PLoS One, 2013. **8**(1): p. e54501.
9. Masola, V., et al., *Heparanase and syndecan-1 interplay orchestrates fibroblast growth factor-2-induced epithelial-mesenchymal transition in renal tubular cells.* J Biol Chem, 2012. **287**(2): p. 1478-88.
10. Boels, M.G.S., et al., *Systemic Monocyte Chemotactic Protein-1 Inhibition Modifies Renal Macrophages and Restores Glomerular Endothelial Glycocalyx and Barrier Function in Diabetic Nephropathy.* Am J Pathol, 2017. **187**(11): p. 2430-2440.
11. Boels, M.G., et al., *Atrasentan Reduces Albuminuria by Restoring the Glomerular Endothelial Glycocalyx Barrier in Diabetic Nephropathy.* Diabetes, 2016. **65**(8): p. 2429-39.
12. Buse, M.G., *Hexosamines, insulin resistance, and the complications of diabetes: current status.* Am J Physiol Endocrinol Metab, 2006. **290**(1): p. E1-E8.
13. Wang, J., et al., *Antioxidant activity of sulfated polysaccharide fractions extracted from Laminaria japonica.* Int J Biol Macromol, 2008. **42**(2): p. 127-32.
14. Yuan, L., et al., *Heparan sulfate mimetic fucoidan restores the endothelial glycocalyx and protects against dysfunction induced by serum of COVID-19 patients in the intensive care unit.* ERJ Open Res, 2022. **8**(2).
15. Buijsers, B., et al., *Glycosaminoglycans and fucoidan have a protective effect on experimental glomerulonephritis.* Front Mol Biosci, 2023. **10**: p. 1223972.
16. Wang, J., et al., *Structural studies on a novel fucogalactan sulfate extracted from the brown seaweed Laminaria japonica.* Int J Biol Macromol, 2010. **47**(2): p. 126-31.
17. Rops, A.L., et al., *Isolation and characterization of conditionally immortalized mouse glomerular endothelial cell lines.* Kidney Int, 2004. **66**(6): p. 2193-201.
18. Maciej-Hulme, M.L., et al., *Glomerular endothelial glycocalyx-derived heparan sulfate inhibits glomerular leukocyte influx and attenuates experimental glomerulonephritis.* Front Mol Biosci, 2023. **10**: p. 1177560.
19. Ridler, T.W. and S. Calvard, *Picture tresholding using an iterative selection method.* IEEE Transactions on Systems, Man, and Cybernetics, 1978. **8**: p. 630-632.

20. Chessa, F., et al., *The renal microenvironment modifies dendritic cell phenotype.* Kidney Int, 2016. **89**(1): p. 82-94.
21. Luthuli, S., et al., *Therapeutic Effects of Fucoidan: A Review on Recent Studies.* Mar Drugs, 2019. **17**(9).
22. Tokita, Y., et al., *Development of a fucoidan-specific antibody and measurement of fucoidan in serum and urine by sandwich ELISA.* Biosci Biotechnol Biochem, 2010. **74**(2): p. 350-7.
23. Smetsers, T.F., et al., *Human single-chain antibodies reactive with native chondroitin sulfate detect chondroitin sulfate alterations in melanoma and psoriasis.* J Invest Dermatol, 2004. **122**(3): p. 707-16.
24. Cao, Q., et al., *Renal F4/80+ CD11c+ mononuclear phagocytes display phenotypic and functional characteristics of macrophages in health and in adriamycin nephropathy.* J Am Soc Nephrol, 2015. **26**(2): p. 349-63.
25. Boels, M.G., et al., *Direct Observation of Enhanced Nitric Oxide in a Murine Model of Diabetic Nephropathy.* PLoS One, 2017. **12**(1): p. e0170065.
26. Regier, M., et al., *A Dietary Supplement Containing Fucoidan Preserves Endothelial Glycocalyx through ERK/MAPK Signaling and Protects against Damage Induced by CKD Serum.* Int J Mol Sci, 2022. **23**(24).
27. Machin, D.R., et al., *Glycocalyx-targeted therapy ameliorates age-related arterial dysfunction.* Geroscience, 2023.

Supplemental

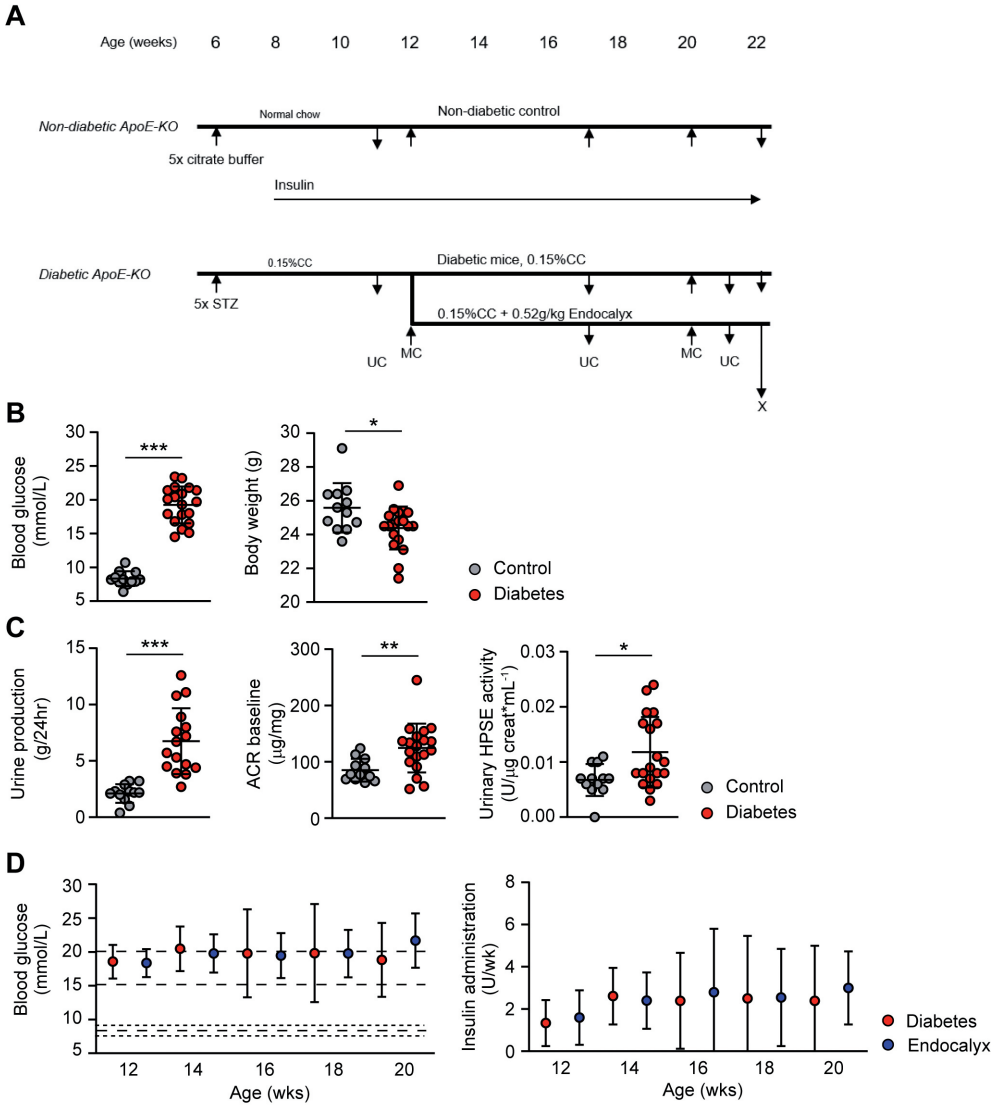

Supplemental figure 1. Design of mouse study and baseline characteristics. (A) Schematic representation of the mouse study. *Abbreviations: STZ = streptozotocin, 0.15%CC = 0.15% cholesterol enriched normal chow, MC = metabolism cage, UC = urine collection. X, endpoint.* Baseline measurements at week 11, before randomization, of **(B)** blood glucose and body weight and **(C)** urine production, albumin-to-creatinine ratio (ACR) and urinary heparanase 1 (HPSE-1) activity of control- and diabetic apoE-KO mice. Averaged weekly **(D)** blood glucose levels and **(E)** insulin administration to maintain preferred blood glucose levels (upper two dashed lines in **D**). **(D)** Lower lines represent mean ± standard deviation blood glucose levels of control apoE-KO mice. Values are given as mean with standard deviation. Differences between groups were assessed by unpaired two-tailed t-test: **P* < 0.05, ***P* < 0.01. ****P* < 0.001.

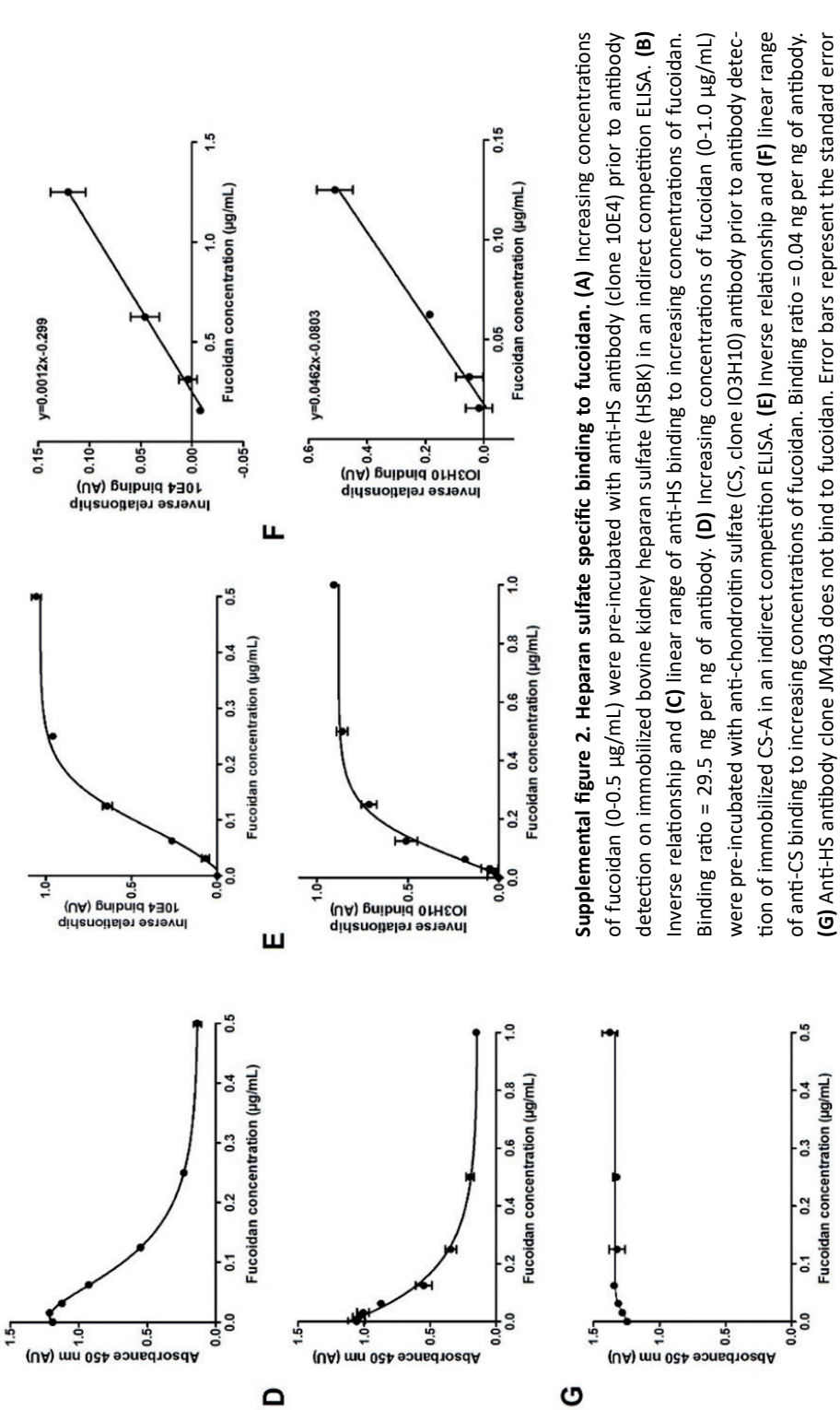

Supplemental figure 2. Heparan sulfate specific binding to fucoidan. (A) Increasing concentrations of fucoidan (0-0.5 µg/mL) were pre-incubated with anti-HS antibody (clone 10E4) prior to antibody detection on immobilized bovine kidney heparan sulfate (HSBK) in an indirect competition ELISA. **(B)** Inverse relationship and **(C)** linear range of anti-HS binding to increasing concentrations of fucoidan. Binding ratio = 29.5 ng per ng of antibody. **(D)** Increasing concentrations of fucoidan (0-1.0 µg/mL) were pre-incubated with anti-chondroitin sulfate (CS, clone IO3H10) antibody prior to antibody detection of immobilized CS-A in an indirect competition ELISA. **(E)** Inverse relationship and **(F)** linear range of anti-CS binding to increasing concentrations of fucoidan. Binding ratio = 0.04 ng per ng of antibody. **(G)** Anti-HS antibody clone JM403 does not bind to fucoidan. Error bars represent the standard error of the mean.

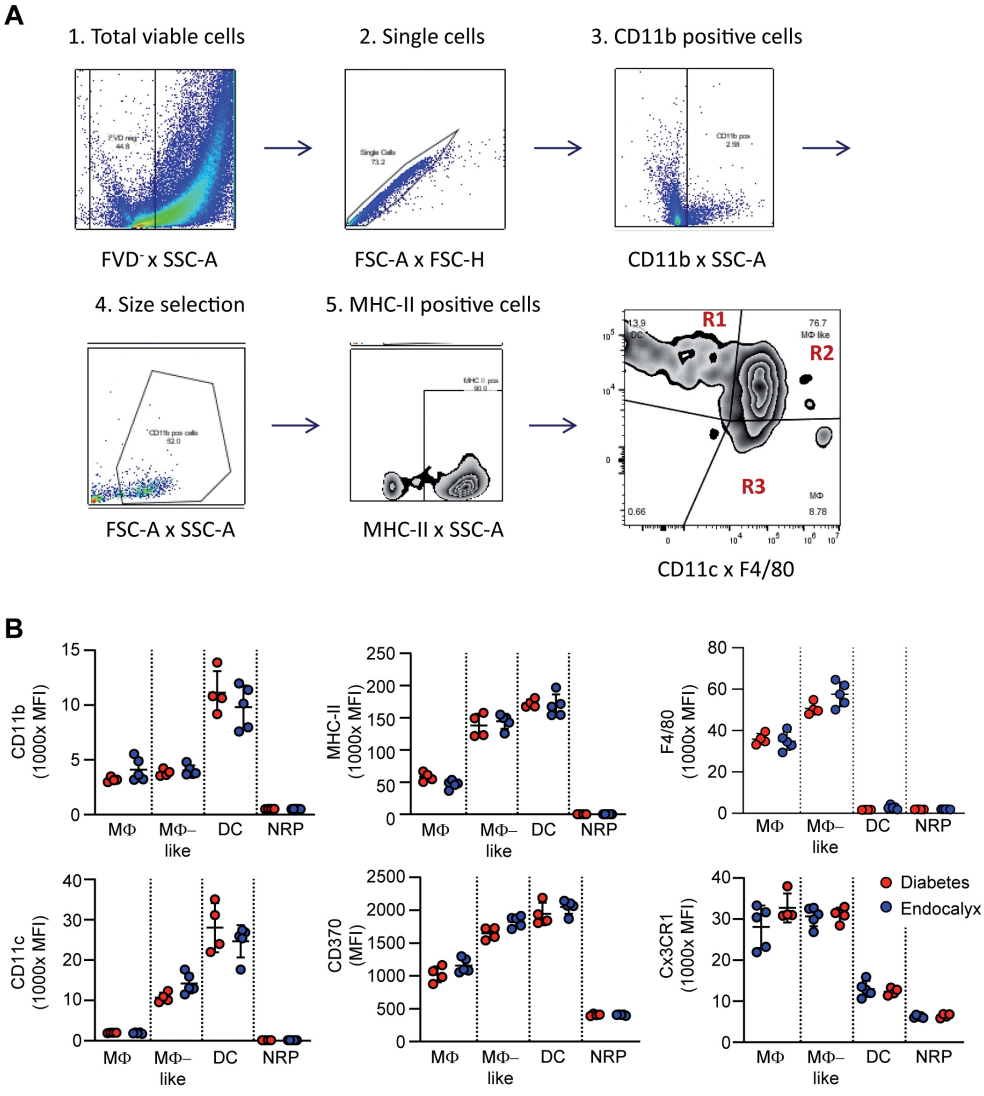

Supplemental figure 3. Cytometry gating strategy for detection of kidney myeloid cells. To determine and stratify renal myeloid cells from total kidney samples. Single cell suspensions, measured on a Cytek Aurora 5 flow cytometer, were gated after **(A)** life/dead discrimination and single cell selection in further steps using CD11b, MHC-II, CD11c and F4/80 as discrimination expression factors which results in a final gate revealing 3 different myeloid cell populations, i.e., dendritic cells (DC: R1), DC with macrophage-like (Mϕ-like) properties (R2) and Mϕ (R3). **(B)** Mean fluorescent intensities (MFI) of CD11b, MHC-II, F4/80, CD11c, DC marker CD307, and the fractalkine receptor Cx3CR1, with respect to the control non-responsive lymphocyte population (NRP).

Supplemental table 1. Reactivity of antibodies with *L. japonica* fucoidan.

Antibody	Known reactivity/epitope[#]	Fucoidan reactivity	Antibody:fucoidan concentration ratio (ng)	R^2
Anti-HS (F58-10E4)[$]	GlcA-GlcNS-GlcA-GlcNAc	yes	1/28.5	0.998
anti-CS scFv (I03H10)	GlcA2S-GalNAc4S6S	yes	1/0.04	0.99
Anti-HS (JM403)	GlcN	no	-	-

[$]Antibody clone number

[#]GlcA, b-D-glucuronic acid; GlcN, glucosamine; GlcNS, 2-deoxy-2-sulfamido-α-D-glucopyranosyl; GlcNAc, N-acetyl-glucosamine; GlcA2S, 2-sulfated b-D-glucuronic acid; GalNAc4S6S, galactosamine-4,6-disulfate

Supplemental table 2. FACScan antibody cocktails.

Marker	Fluorochrome	Concentration (µg/mL)	Company[#]	Cat no.
Tubes 1-4 (extracellular)				
FVD[$]	eFlour780		eBioscience	65-0865-18
F4/80	SuperBright 436	10	eBioscience	62-4801-82
CX3CR1	BV510	1.3	Biolegend	149025
MHC-II	AF700	5.0	Biolegend	107622
CD11b	PerCP	1.0	Biolegend	101230
CD11c	APC	4.0	BD	550261
CD370 (Clec9a)	AF594	5.0	R&D	FAB67761T
Tube 1 (intracellular), control				
Rabbit IgG	AF488	5.0	eBioscience	53-4616-82
Tube 2 (intracellular)				
Heparanase	AF488	5.0	Bioss Antibodies	BS-1541R-A488
Tube 3 (intracellular), control				
Rabbit IgG	-	20	Dako	X0903
Tube 4 (intracellular)				
Cathepsin L	-			

[$]FVD, fixable viability dye

[#] eBioscience, Thermo Fisher Scientific, Amsterdam, The Netherlands; Biolegend, San Diego, CA, USA; BD Biosciences, Vianen, The Netherlands; R&D Systems, Abingdon, UK; Bioss Antibodies, Woburn, MA, USA; Dako, Agilent Technologies Netherlands B.V., Amstelveen, The Netherlands